Mode II Edge Delamination of Compressed Thin Films

D. S. Balint
Assoc. Mem. ASME

J. W. Hutchinson
Fellow ASME

Division of Engineering and Applied Sciences,
Harvard University,
Cambridge, MA 02138

Ceramic coatings deposited on metal substrates generally develop significant compressive stresses when cooled from the temperature at which they are processed as a result of thermal expansion mismatch. One of the main failure modes for these coatings is edge delamination. For an ideally brittle interface, the edge delamination of a compressed thin film involves mode II interface cracking. The crack faces are in contact with normal stress acting across the faces behind the advancing tip. Frictional shielding of the crack tip has been shown to increase the apparent fracture toughness. Roughness effects associated with the separating faces can also contribute to the apparent toughness. A model of mode II steady-state edge delamination that incorporates combined friction and roughness effects between the delaminated film and substrate is proposed and analyzed. This model is used to assess whether frictional shielding and surface roughness effects are sufficient to explain the large apparent mode II fracture toughness values observed in experiments.
[DOI: 10.1115/1.1388012]

1 Introduction

Many thin film manufacturing techniques create residual stresses in the film that can lead to failure. Ceramic coatings deposited on metal substrates generally develop significant compressive stresses as a result of thermal expansion mismatch when cooled from the temperature at which they are processed. Systems of this type are of interest as thermal barrier and wear coatings. Two of the primary failure modes for films in compression are edge delamination and buckle delamination (c.f. Fig. 1). The elastic energy per unit area stored in the film which is available upon edge delamination is

$$\mathcal{G}_0=\frac{(1-\nu^2)\sigma^2 h}{2E} \tag{1}$$

where E and ν are the Young's modulus and Poisson's ratio of the film, h is the film thickness, and σ is the uniform compressive biaxial prestress in the film. To a first approximation, $\mathcal{G}_0$ is also the energy available to drive the interface delamination crack for buckle delaminations. The typical flaw size (in the form of a debonded region) needed to initiate a buckle delamination is about $20h$. Delaminations that emanate from a film edge and terminate in the interior of the substrate surface only require debond flaws as small as 1 or $2h$ for initiation ([1]). This would suggest that edge delaminations would be more commonly observed than buckle delaminations. In fact, the opposite is true. Many systems seem to fail primarily by buckle delaminations initiated away from the edges of the film.

There are many reasons why edge delaminations are less common than might be expected. Edge delamination is a mode II cracking phenomenon when the film is in compression, and it is now well known that mode II tends to be associated with the highest interface toughness. By contrast, buckle delamination is mixed mode but approaches mode II as the delamination spreads and arrests ([2]). In addition, there are extrinsic effects accompanying mode II edge delamination which contribute to the apparent toughness. Frictional sliding is one such effect ([3]). Another, which is the primary focus of this paper, is the effect that surface roughness has on the delaminated film as it slides over the substrate. The roughness forces open the film-substrate interface as the delamination crack faces displace, resulting in normal stresses at the interface that are larger than those produced in the absence of roughness. This leads to greater frictional dissipation and shielding of the crack tip. At the same time, however, it can also wedge open the crack tip producing a mode I stress intensity component. Most failed interfaces have a characteristic roughness. The present study suggests that frictional sliding *and* wedging due to roughness should generally be considered in combination in problems such as this. Specifically, it will be shown that nanoscale roughness has a significant influence on the effective mode II toughness of films whose thickness is in the micron range.

Contributed by the Applied Mechanics Division of THE AMERICAN SOCIETY OF MECHANICAL ENGINEERS for publication in the ASME JOURNAL OF APPLIED MECHANICS. Manuscript received by the ASME Applied Mechanics Division, September 7, 2000; final revision, March 3, 2001. Associate Editor: H. Gao. Discussion on the paper should be addressed to the Editor, Professor Lewis T. Wheeler, Department of Mechanical Engineering, University of Houston, Houston, TX 77204-4792, and will be accepted until four months after final publication of the paper itself in the ASME JOURNAL OF APPLIED MECHANICS.

2 Formulation of the Model

2.1 Modeling the Delaminated Interface. We study steady-state edge delamination of a thin film of thickness h with shear modulus $\mu=E/(2(1+\nu))$ and Poisson's ratio ν that is in uniform residual compression and is bonded to a very thick sub-

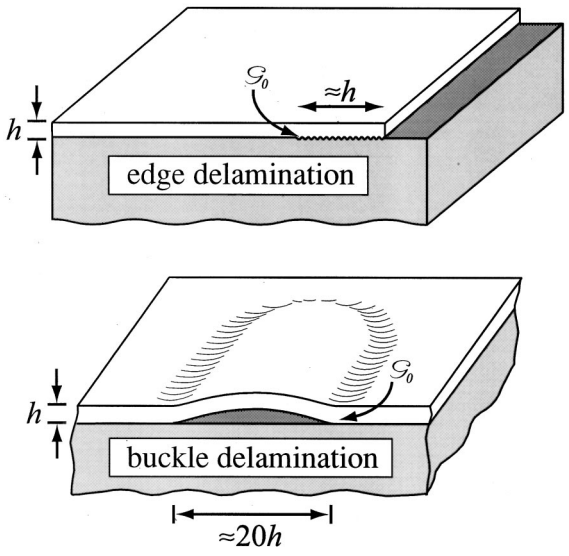

Fig. 1 A schematic showing an edge delamination and a buckle delamination and the minimum flaw sizes necessary to achieve steady-state

 Copyright © 2001 by ASME

strate having the same elastic properties. Stringfellow and Freund [3] showed that the effect of elastic mismatch between film and substrate is secondary to the role of friction. The same is expected for the roughness effect studied here, and thus an investigation of the role of dissimilar materials is postponed. The delamination is assumed to have propagated away from the edge a distance that is much larger than the film thickness, such that h is the only relevant length scale. Friction and roughness effects are significant mainly within a few film thicknesses of the interfacial crack tip, so the film-substrate system can be modeled as an elastic half-space with a thin film perfectly bonded along half of its length and fully delaminated along the other half. Under plane strain conditions the problem reduces to a two-dimensional one where the film is in a state of uniform compression far ahead of the interfacial crack tip and is stress free far behind the crack tip.

Using the superposition scheme shown in Fig. 2, the problem of interest (c.f. Fig. 2(a)) can be decomposed into the problem depicted in Fig. 2(b) and the reduced problem shown in Fig. 2(c). Note that there is no displacement of the film relative to the substrate for the problem shown in Fig. 2(b). This can be understood by imagining a film that is under uniform compression and then is debonded along half of its length with a compressive stress applied remotely to hold it in place. Since the displacement is zero, the stress intensity is also zero. Thus the displacement and stress intensity for the problem of interest are identical to those for the reduced problem. It is the reduced problem that is solved in this paper.

Roughness on a scale that is small relative to the film thickness is assumed to be present at the interface between the delaminated film and the substrate. Specifically, the results which emerge from the present study suggest that roughness on the order of one hundredth the film thickness or even somewhat smaller has the largest effect on the apparent energy release rate. The roughness is assumed to be random on the delaminated interface such that once sliding across the interface has occurred on the order of one roughness half-wavelength l, the two surfaces become uncorrelated and are thereafter propped open a distance R, the amplitude of the roughness. This is depicted in Fig. 3, although the influence of the two-dimensionality of the roughness is not portrayed.

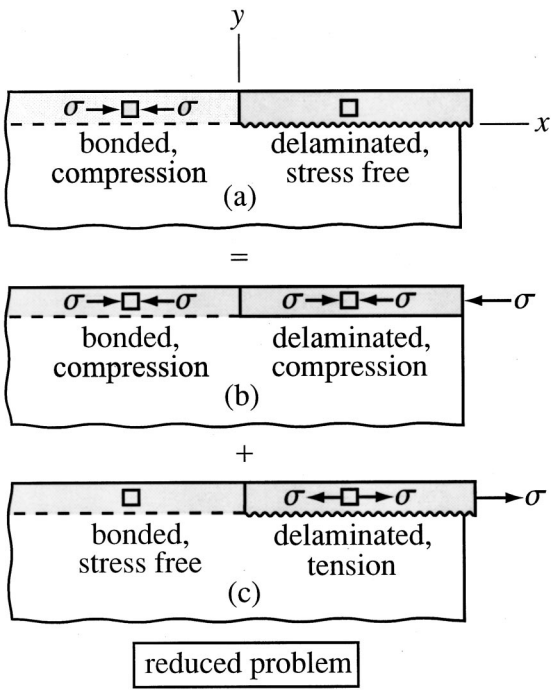

Fig. 2 A schematic of the superposition scheme

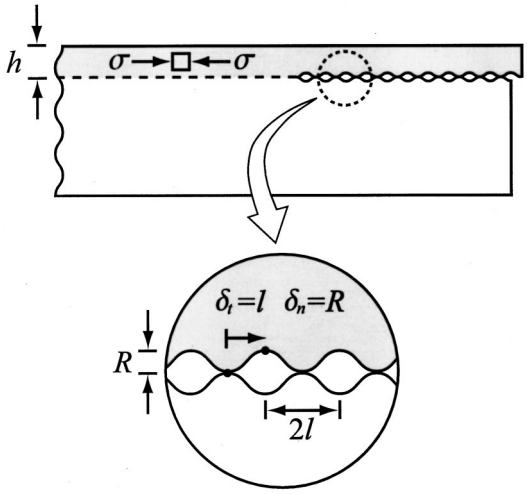

Fig. 3 The coupling of normal and tangential displacements caused by surface roughness

To model the roughness, the relative normal displacement of the two surfaces, δ_n, is assumed to be related to the relative tangential displacement of the two surfaces, δ_t, by

$$\delta_n(s) = R(1 - e^{-\delta_t(s)/l}), \tag{2}$$

which is plotted in Fig. 4. We retain the assumption of Coulomb friction at the interface such that on a scale that is large relative to l, but small compared to h

$$\sigma_{xy}(x) = -\mu_f \sigma_{yy}(x) \quad x > 0, \tag{3}$$

when sliding occurs. Thus, the rough interface is replaced by a planar crack where the two components of crack-face displacement are constrained by (2) and the two components of traction are constrained by (3).

Conditions must be imposed to ensure that the solution is consistent with the sign of the friction condition: (i) the normal stress behind the delamination crack tip must be compressive and (ii) the tangential displacement must be a monotonically increasing function of distance behind the tip. The latter of these conditions ensures that the sliding is in one direction under the steady-state propagation.

2.2 Integral Equation Formulation. As already noted, the solution to the problem in Fig. 2(b) makes no contribution to the stress intensity factors. The reduced problem shown in Fig. 2(c) is formulated and solved thereby providing the stress intensity fac-

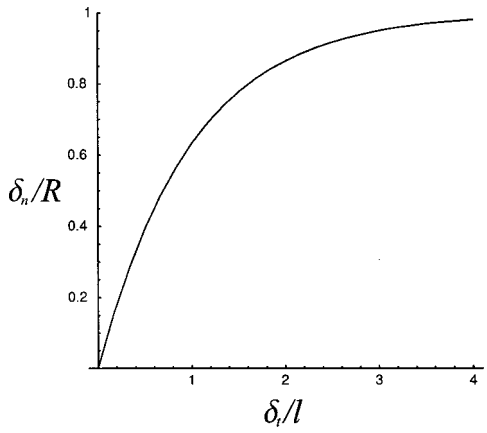

Fig. 4 A plot of the displacement coupling relationship

tors for the problem in Fig. 2(*a*). The interfacial crack between the film and the substrate is equivalent to a continuous distribution of elastic edge dislocations ([4]). A single elastic edge dislocation a distance h below the free surface of the half-space (i.e., on the x-axis of the coordinate system depicted in Figure 2(*a*)) creates a stress field in the surrounding material that is given by the Airy stress function:

$$\Phi=\frac{\mu}{2\pi(1-\nu)}\left\{\frac{2b_y x(h-y)+b_x[x^2+(2h-y)y]}{x^2+(2h-y)^2}h + \frac{b_y x-b_x y}{2}\log\left[\frac{x^2+y^2}{x^2+(2h-y)^2}\right]\right\}, \tag{4}$$

where (b_x, b_y) is the Burger's vector for the dislocation (a factor of two missing from the expression for Φ given by Stringfellow and Freund has been incorporated here) ([3,5]). The stress field for a single edge dislocation located at a position s on the x-axis can be derived from Eq. (4). With

$$\beta_x(s)=\frac{d\delta_t(s)}{ds} \tag{5}$$

$$\beta_y(s)=\frac{d\delta_n(s)}{ds} \tag{6}$$

on the x-axis a distance x behind the crack tip, the stresses are given in terms of the dislocation distribution $(\beta_x(s),\beta_y(s))ds$ by

$$\sigma_{xy}(x)=\frac{\mu}{2\pi(1-\nu)}\left[\int_0^\infty \frac{g_{11}(\xi)}{\xi}\beta_x(s)ds+\int_0^\infty g_{12}(\xi)\beta_y(s)ds\right], \tag{7}$$

$$\sigma_{yy}(x)=\frac{\mu}{2\pi(1-\nu)}\left[\int_0^\infty g_{21}(\xi)\beta_x(s)ds+\int_0^\infty \frac{g_{22}(\xi)}{\xi}\beta_y(s)ds\right], \tag{8}$$

where $\xi=x-s$ and

$$g_{11}(\xi)=\frac{64h^2+16h^4\xi^2+16h^2\xi^4}{(4h^2+\xi^2)^3}, \tag{9}$$

$$g_{12}(\xi)=\frac{-32h^5+24h^3\xi^2}{(4h^2+\xi^2)^3}, \tag{10}$$

$$g_{21}(\xi)=\frac{32h^5-24h^3\xi^2}{(4h^2+\xi^2)^3}, \tag{11}$$

$$g_{22}(\xi)=\frac{64h^6-48h^4\xi^2}{(4h^2+\xi^2)^3}. \tag{12}$$

The single governing integral equation expressed with $\beta_x(s)$ as the unknown is obtained by imposing Eq. (3):

$$\int_0^\infty \frac{g_{11}(\xi)}{\xi}\beta_x(s)ds+\int_0^\infty g_{12}(\xi)\beta_y(s)ds = -\mu_f\left[\int_0^\infty g_{21}(\xi)\beta_x(s)ds+\int_0^\infty \frac{g_{22}(\xi)}{\xi}\beta_y(s)ds\right], \tag{13}$$

where from Eqs. (2) and (6),

$$\beta_y(s)=\frac{R}{l}\beta_x(s)\exp\left[-\frac{1}{l}\int_0^s \beta_x(\eta)d\eta\right]. \tag{14}$$

It is known from linear elastic fracture mechanics that $\beta_x(s)$ has a $s^{-1/2}$ singularity at the crack tip. Far behind the tip the film is in a state of plane strain extension. These conditions are described as

$$\beta_x(s)\propto\frac{1}{\sqrt{s}} \text{ as } s\to 0, \tag{15}$$

$$\beta_x(s)\to\frac{\sigma(1-\nu^2)}{E} \text{ as } s\to\infty. \tag{16}$$

The stress intensity factors are given by

$$K_I=\lim_{s\to 0}\frac{\sqrt{2\pi s}}{4}\frac{E}{1-\nu^2}\beta_y(s), \tag{17}$$

$$K_{II}=\lim_{s\to 0}\frac{\sqrt{2\pi s}}{4}\frac{E}{1-\nu^2}\beta_x(s). \tag{18}$$

Note that by Eq. (14) that as $s\to 0$,

$$\beta_y(s)\to\frac{R}{l}\beta_x(s), \tag{19}$$

therefore the mode mix is fixed according to

$$K_I=\frac{R}{l}K_{II}. \tag{20}$$

The mode II stress intensity factor for a steady-state edge delamination with zero friction and no roughness is

$$K_{II}^0=\sigma\sqrt{\frac{h}{2}}, \tag{21}$$

and the energy release rate is given by Eq. (1). Normalizing by these values and applying

$$\mathcal{G}=\frac{1-\nu^2}{E}(K_I^2+K_{II}^2), \tag{22}$$

yields the following relationships for the energy release rate:

$$\frac{\mathcal{G}}{\mathcal{G}_0}=\left(\frac{K_{II}}{K_{II}^0}\right)^2\left[1+\left(\frac{R}{l}\right)^2\right]. \tag{23}$$

The dimensionless equation shown in the Appendix reveals that the solution is determined by three dimensionless parameters, i.e.,

$$\frac{K_{II}}{K_{II}^0}=f\left(\bar{\sigma}=\frac{\sigma h(1-\nu^2)}{El},\bar{R}=\frac{R}{l},\mu_f\right). \tag{24}$$

Further details of the formulation, along with aspects of the numerical solution scheme, are presented in the Appendix.

3 Results

The combined effect of friction and roughness on the mode II stress intensity factor is shown in Fig. 5. There, plots of K_{II}/K_{II}^0 as a function of $\bar{\sigma}$ are presented for various roughness levels and two values of the coefficient of friction. When friction is present without any roughness, the normalized stress intensity factor is independent of the film stress. Its reduction below the frictionless limit $(K_{II}/K_{II}^0=1)$ is relatively small and is precisely in accord with the results of Stringfellow and Freund [3]. Combined friction and roughness lead to a dependence of the stress intensity factor on $\bar{\sigma}$ such that the full effect of the roughness is attained when $\bar{\sigma}\approx 2$. For $\bar{\sigma}\geq 2$, the effect of roughness on K_{II} is pronounced. Values of R/l as large as unity cannot be ruled out and, indeed, are to be expected when one or both of the materials are polycrystalline.

The effect of friction and roughness on the normalized energy release rate from Eq. (23) is plotted in Fig. 6 for the same two values of μ_f. The competition between the reduction in K_{II} due to combined friction and wedging and the increase in K_I due to wedging (c.f. Eq. (14)) is evident. At sufficiently small $\bar{\sigma}$, $\mathcal{G}/\mathcal{G}_0$ is increased above the zero roughness limit due to the dominant influence of wedging on K_I. For $\mu_f=.5$, $\mathcal{G}/\mathcal{G}_0$ exceeds the zero

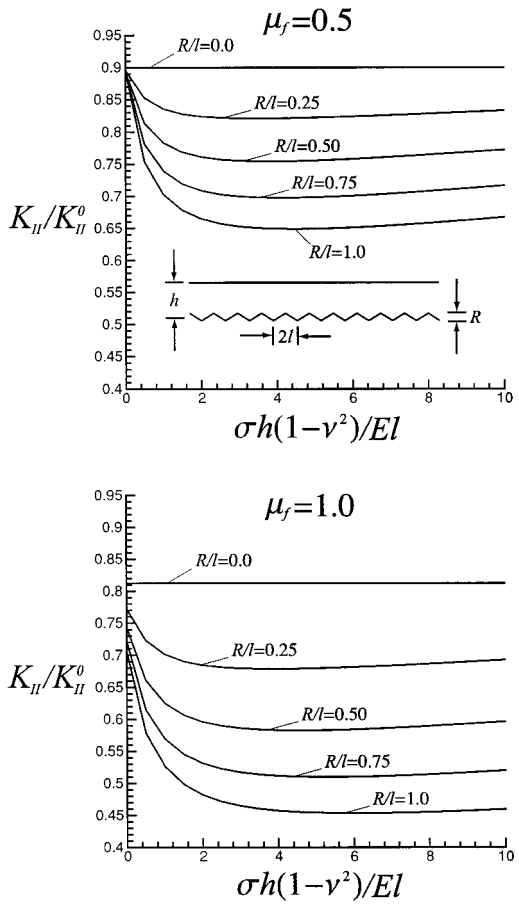

Fig. 5 Normalized mode II stress intensity factor

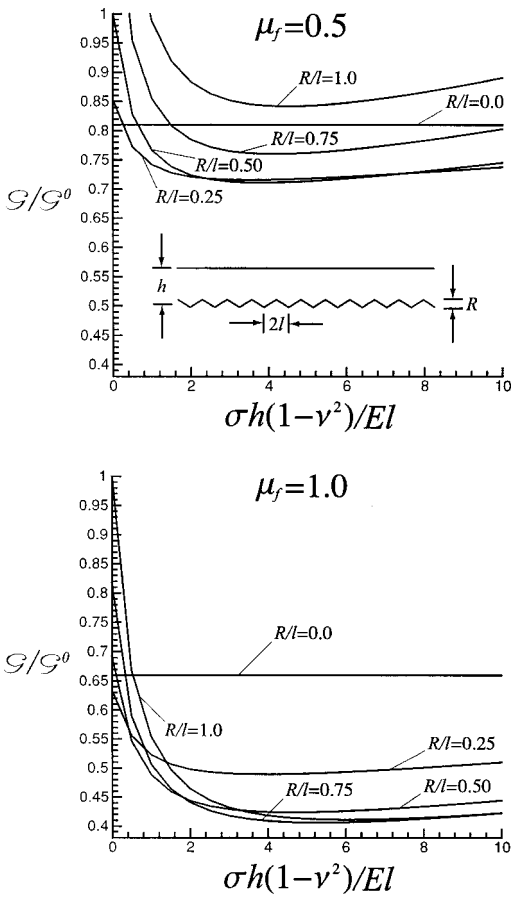

Fig. 6 Normalized energy release rate

roughness limit for all $\bar{\sigma}$ if $R/l=1$. However, it is apparent that there is a significant range of R/l and $\bar{\sigma}$ such that the combined effect of friction and roughness reduces $\mathcal{G}/\mathcal{G}_0$ by approximately twice the effect of friction alone. For $\mu_f=.5$, the maximum crack-tip shielding corresponds to $\mathcal{G}/\mathcal{G}_0\approx.7$ for a roughness level $R/l\approx.5$ and $\bar{\sigma}>2$. For $\mu_f=1$, the corresponding value is $\mathcal{G}/\mathcal{G}_0\approx.4$.

Examples of the normal stress distribution acting on the interface behind the crack tip are given in Fig. 7. Roughness increases the normal stress within a distance of about one film thickness from the tip. It is this increase which provides greater frictional dissipation and thereby diminishes the mode II stress intensity factor. The normal stress becomes very slightly negative along part of the interface at $x/h>5$, but its magnitude is so small that there is no need to extend the formulation to account for a segment of the interface that is open. This condition has been checked for the full range of parameters governing the solution. In addition, the monotonicity condition for the tangential crack displacement, which is necessary for consistency of the imposed friction condition, was satisfied.

The reduction in the energy release rate (c.f. Fig. 6) gives further insight into the combined effect of friction and interface roughness. The simplest possible condition for crack advance based on crack-tip stress intensity would be the mode-independent criterion

$$\mathcal{G}=\Gamma_0 \tag{25}$$

where Γ_0 is considered as the separation energy for the interface. Then, the apparent mode II toughness for steady-state propagation would be $\Gamma\equiv\mathcal{G}_0$ since $\mathcal{G}_0$ is the overall energy release rate. Using the results of Fig. 6, one can plot the normalized apparent mode II toughness, Γ/Γ_0, as is done in Fig. 8 for $R/l=.5$.

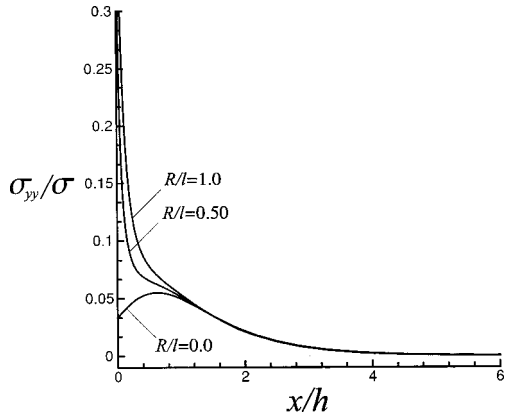

Fig. 7 Normal stress at the interface for $\mu_f=1.0$ and $\bar{\sigma}=5.0$

4 Concluding Remarks

Results of this study indicate that the mechanism of combined frictional sliding and roughness-wedging has an effect on the apparent mode II fracture toughness that can be as much as twice the effect of friction alone. Toughness values as large as 2.5 times the separation energy of the interface were predicted. The stress intensity at the crack tip was found to decrease significantly with an increase in the amplitude of the roughness. It was also found that the presence of roughness at the interface induces a mode I stress intensity that is at most equal to the mode II stress intensity for the

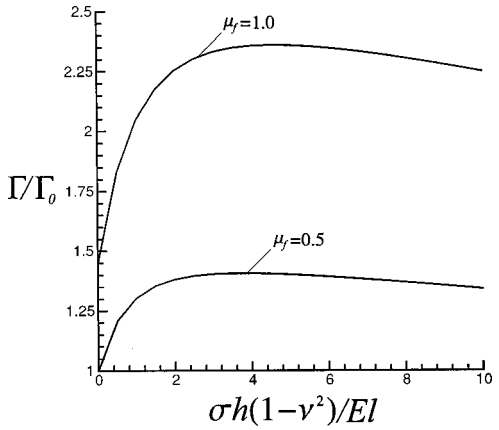

Fig. 8 Normalized apparent mode II fracture toughness for $\bar{R}$ =0.5

range of roughness parameter values considered. Thus, what is generally considered a pure mode II phenomenon is in fact mixed mode at the tip when the interface is rough.

In addition to the roughness parameter, the analysis revealed that the normalized energy release rate depends on one important dimensionless stress parameter, $\bar{\sigma}=\sigma h(1-\nu^2)/El$. Consider a film whose thickness is about one micron and supports a stress to modulus level of about .01. A roughness half-wavelength, l, on the order of ten nanometers would produce a value of $\bar{\sigma}$ large enough to significantly affect the apparent interface toughness. Such a wavelength is fully consistent with the underlying assumptions of the model and the analysis.

Previous models that considered only frictional sliding showed that material mismatch can further increase the apparent mode II fracture toughness when the film is more compliant than the substrate ([3]). It is expected that the same trend would be observed when roughness effects are considered in combination with frictional sliding for the bimaterial problem, yielding apparent mode II fracture toughness values even larger than those predicted by this study. For an interface with an array of contacting asperities, a more realistic representation of the coefficient of friction can be expressed as the sum of a constant term and a term that is proportional to the dilatancy of the interface ([6]). For the roughness model assumed in this paper, the dilatancy term is positive. Thus incorporating a more realistic friction model would result in additional frictional dissipation and a corresponding increase in the apparent mode II toughness. The results of this model in conjunction with these additional mechanisms that enhance the toughness shows that it is indeed possible to predict mode II toughness values that begin to become comparable to those found in experiments by modeling the combined effect of frictional sliding and roughness-wedging at the interface. Furthermore, the strong coupling between frictional sliding and roughness-wedging shows that both effects should be considered in combination when modeling the delamination of compressed thin films.

Acknowledgment

This work was supported in part by a grant entitled ''Prime Reliant Coatings'' from the Office of Naval Research, by the National Science Foundation (CMS-96-34632), and by the Division of Engineering and Applied Sciences. Daniel S. Balint acknowledges the support of the National Defense Science and Engineering Graduate Fellowship Program.

Appendix

To facilitate numerical solution, the domain of integration is transformed from $s,x\in[0,\infty)$ to $t,z\in[-1,1]$ by setting

$$s=h\frac{1+t}{1-t}$$

and

$$x=h\frac{1+z}{1-z}.$$

When the displacement coupling relationship given by Eq. (2) is used, Eq. (13) can be expressed in terms of dimensionless variables as

$$\int_{-1}^{1}\beta(t)\left\{\frac{k_{11}(z,t)(1-z)}{(z-t)(1-t)}+2\mu_f\frac{k_{21}(z,t)}{(1-t)^2}\right\}dt = -\bar{R}\int_{-1}^{1}\beta(t)\exp[-\bar{\sigma}\delta(t)]\left\{2\frac{k_{12}(z,t)}{(1-t)^2}+\mu_f\frac{k_{22}(z,t)(1-z)}{(z-t)(1-t)}\right\}dt, \tag{26}$$

for the unknown

$$\beta(t)=\frac{E}{\sigma(1-\nu^2)}\beta_x\left(h\frac{1+t}{1-t}\right), \tag{27}$$

where

$$\bar{R}=\frac{R}{l}, \tag{28}$$

$$\bar{\sigma}=\frac{\sigma h(1-\nu^2)}{El}, \tag{29}$$

$$\delta(t)=\frac{E}{\sigma(1-\nu^2)}\int_{-1}^{t}\beta_x\left(h\frac{1+\tau}{1-\tau}\right)\frac{2}{(1-\tau)^2}d\tau, \tag{30}$$

$$k_{11}(z,t)=g_{11}\left(h\frac{2(z-t)}{(1-z)(1-t)}\right), \tag{31}$$

$$k_{12}(z,t)=g_{21}\left(h\frac{2(z-t)}{(1-z)(1-t)}\right)h, \tag{32}$$

$$k_{21}(z,t)=g_{12}\left(h\frac{2(z-t)}{(1-z)(1-t)}\right)h, \tag{33}$$

$$k_{22}(z,t)=g_{22}\left(h\frac{2(z-t)}{(1-z)(1-t)}\right). \tag{34}$$

The dimensionless end conditions are expressed as

$$\beta(t)\propto\frac{1}{\sqrt{1+t}}\ \text{ as }\ t\to-1, \tag{35}$$

$$\beta(t)\to 1\ \text{ as }\ t\to 1. \tag{36}$$

Any real continuous function defined on the interval $[-1, 1]$ can be approximated by a finite linear combination of Chebyschev polynomials of the first kind. Thus the dislocation density can be expressed as

$$\beta(t)=\frac{1}{\sqrt{1+t}}\left[\sqrt{2}+(1-t)\sum_{n=1}^{N}a_nT_{n-1}(t)\right], \tag{37}$$

where the integer N is adjusted to achieve the desired accuracy and the expansion coefficients a_n are unknown. Both boundary conditions are satisfied by this form. Substituting Eq. (37) into Eq. (26) yields an integral equation involving the N unknown expansion coefficients that must be satisfied for all $z\in[-1,1]$. Satisfying the integral equation at N values of z produces an $N\times N$ linear system $\mathbf{Ax}=\mathbf{b}$ where the components of the $N\times 1$ vector $\mathbf{x}$ are the expansion coefficients. This linear system can be solved for the

unknown coefficients which can then be used to construct the dislocation density, stress intensity factors, and energy release rate.

The components of the $N \times N$ matrix **A** and the $N \times 1$ vector **b** are singular integrals, the integrands of which are expressible in a form that permits numerical evaluation using Gauss-Chebyschev sums for singular integrals derived by Erdogan and Gupta [7]. Convergence must be achieved for the individual Gauss-Chebyschev sums used to evaluate the integrals by choosing the number of terms in each sum, M, sufficiently large and for the Chebyschev expansion by choosing N sufficiently large. Numerical error in the linear system increases with N and for some N surpasses the accuracy gained. Thus an optimal value of N exists and was determined.

The Gauss-Chebyschev sums can only be evaluated at the zeros of the $(M-1)$th Chebyschev polynomial of the second kind. If $M/2N$ is a positive integer, the zeros of the Nth Chebyschev polynomial of the first kind are a subset of the zeros of the $(M-1)$th Chebyschev polynomial of the second kind. This fact was utilized to evaluate the Gauss-Chebyschev sums at the zeros of the Nth Chebyschev polynomial of the first kind, which was the only set of N values of z for which good convergence was found. Convergence to six decimal places was achieved for $N=12$ and $M=48{,}000$ for the case where $\mu_f=0$ and $\bar{R}=0$ which has a known analytical solution. These values of N and M were used for all subsequent calculations involving nonzero μ_f and $\bar{R}$.

References

[1] Yu, H., He, M. Y., and Hutchinson, J. W., 2001, "Edge Effects in Thin Films," Acta Mater., in print.

[2] Hutchinson, J. W., and Suo, Z., 1992, "Mixed Mode Cracking in Layered Materials," Adv. Appl. Mech., **29**, pp. 63–191.

[3] Stringfellow, R. G., and Freund, L. B., 1993, "The Effect of Interfacial Friction on the Buckle-Driven Spontaneous Delamination of a Compressed Thin Film," Int. J. Solids Struct., **30**, pp. 1379–1395.

[4] Rice, J. R., 1968, "Mathematical Analysis in the Mechanics of Fracture," Fracture, **2**, pp. 191–311.

[5] Dundurs, J., 1969, "Elastic Interaction of Dislocations With Inhomogeneities," *Mathematical Theory of Dislocations*, ASME, New York, pp. 70–115.

[6] Scott, R. F., 1963, *Principles of Soil Mechanics*, Addison-Wesley, Reading, MA.

[7] Erdogan, F., and Gupta, G. D., 1972, "On the Numerical Solution of Singular Integral Equations," Quart. Appl. Math., pp. 525–534.